RSC Publishing Faraday Discussions

FDASSEMBLY Structural Characterization of Aqueous Solutions Poly(oligo(ethylene oxide) monomethyl methacrylate) - grafted Silica Nanoparticles

Journal:	*Faraday Discussions*
Manuscript ID	FD-ART-09-2015-000137.R1
Article Type:	Paper
Date Submitted by the Author:	13-Oct-2015
Complete List of Authors:	Krishnamoorti, Ramanan; University of Houston, Chemical and Biomolecular Engineering Chatterjee, Tirtha; The DOw Chemical Company, Ponnapati, Ramakrishna; University of Houston, Chemical and Biomolecular Engineering Lorenzo, Arnaldo; University of Houston, Chemical and Biomolecular Engineering

Structural Characterization of Aqueous Solutions Poly(oligo(ethylene oxide) monomethyl methacrylate) - grafted Silica Nanoparticles

Arnaldo T. Lorenzo, Ramakrishna Ponnapati, Tirtha Chatterjee, Ramanan Krishnamoorti*

Department of Chemical and Biomolecular Engineering,
University of Houston, Houston, TX 77204.

Abstract

The structure of aqueous dispersions of poly(oligo(ethylene oxide) monomethyl methacrylate) grafted silica nanoparticles was characterized using contrast variation small-angle neutron scattering studies. Modeling the low hybrid concentration dispersion scattering data using a fuzzy sphere and a polydisperse core – shell model, demonstrated that the polymer chains are highly swollen in the dispersions as compared to the dimensions of free polymer chains in dilute solution. At higher hybrid concentrations, the dispersions were well described using a Percus – Yevick approximation to describe the structure factor. These structural characterization tools are excellent starting points for the effective molecular level descriptors of dewetting and macroscopic phase transitions for polymer tethered hybrid nanoparticle systems.

*Corresponding Author: ramanan@uh.edu

Introduction

Grafting polymers onto solid surface is attracting significant interest due to their important applications ranging from colloidal stabilizers to nanocomposite materials [1, 2]. Polymer-*graft*ed nanoparticles, with core–shell morphologies, can offer promising properties for applications in many varied fields [3]. Core–shell structured materials display a monomer density profile that decays from the particle center to its periphery and might provide superior properties useful for many applications, as for example, in controlled release or sensors [4], or solution rheology modifiers [5].

The "grafting-from" technique is commonly used to covalently attach vinyl polymers by conventional free radical polymerization in conjunction with surface-bound initiators [6, 7]. However, this approach cannot provide a good control over the molecular weight, polydispersity, and terminal chain functionality of the grafted polymers. The aforementioned problem can be reduced by the use of more controlled "living-like" polymerization methods where control over molecular weight, polydispersity, and structure of the resulting polymer can be attained [8]. Atom transfer radical polymerization (ATRP) [8, 9] has proven to be a versatile approach for incorporating (grafting) organic (co)polymers of precise molar mass, composition, and functionality onto surface [6, 10] and substrates [4, 11].

Synthesis of poly(oligo(ethylene oxide) monomethyl methacrylate) (POEOMA) polymers with various structures remains an active research area [12]. Self-assembly of brush-like POEOMA homopolymers were investigated in aqueous solutions by employing dynamic/static light scattering and transmission electron microscopy (TEM) [13]. The thermoresponsive behavior of POEOMA has been explored extensively for possible temperature triggered encapsulation and release applications [14]. Moreover, POEOMA was copolymerized with other polymers such as methacrylic acid[15] and ethyl cellulose[16] to create materials with unique properties. Ion-sensitive

responsive polymers were made to allow a phase transition to be triggered without a temperature change[17]. Copolymers with both thermoresponsive and photocrosslinkable properties were prepared using ATRP [18]. The copolymers can be crosslinked by photopolymerization through their multivinyl functional groups. Linear copolymers or 4-arm star-block copolymers have also been prepared with permanently hydrophilic poly(ethylene oxide) (PEO) inner blocks and thermoresponsive POEOMA outer blocks [19].

In the present paper we present a comprehensive investigation by small-angle neutron scattering (SANS) of the structure of aqueous solutions of POEOMA-grafted silica nanoparticles [20]. Much interest has focused on understanding the structure of polymer chains in such hybrid materials [2, 21, 22-24] as the issues of wetting and de-wetting from such brush geometries have not been completely worked out [1, 25, 26]. A direct modeling expression for the scattering intensity profiles is presented and evaluated, which describes the experimental scattering intensity, *I(q) vs.* wavevector, *q,* data over a broad range of *q*, at different solvent isotopic ratios (different D_2O/H_2O mixture compositions). Using this model, the Fuzzy Sphere model[27], the structure of the nanoparticles (core and shell sizes relationship) can be obtained and analyzed. These efforts parallel those performed on other grafted nanoparticle systems[28, 29, 30, 31] and previous efforts to understand the chain conformations of multi-arm stars[30, 32, 33] and dendrimers[34] in solution. Moreover, for conditions where the polymer shell is poorly contrasted with the solvent, a simple core – shell model was employed model the neutron scattering results. The understanding of the structure of the nanoparticle – polymer hybrid dispersions is a crucial first step towards elucidating the structure and structural transitions in polymer matrices and the influence of thermodynamic interactions on these properties [35]. Two significant problems of interest include the understanding the changes in brush structure as a result of a changing thermodynamic quality

of a matrix (or solvent)[35] and the impact of the brush structure on the effective interfacial activity of such hybrid nanoparticles in oil – water mixtures [23].

Materials and Methods

Materials: 11-Bromo-1-undecanol (98%), 2-Bromo-2-methyl propionyl bromide (98%), diethyl ether (99+%), magnesium sulfate ($MgSO_4$ anhydrous, 97+%), methanol (MeOH, 99.8%), copper(I) bromide (CuBr, 98%), tetrahydrofuran (THF, 99+%) and cyclohexane (99+%) from Sigma-Aldrich, 2,2' bipyridyl (98+%) and anisole (99+%) from Fluka, trimethyl amine (33wt% solution in EtOH) from Acros Organics, were used as received without further purification. Colloidal silica (SiO_2, 47-49wt% in H_2O) was kindly supplied by Nissan Chemicals and was also used as received. Poly(ethylene glycol) methyl ether methacrylate (OEOMA475) was purchased from Sigma-Aldrich and passed through a column packed with alternating layers of inhibitor removers for hydroquinone (HQ), hydroquinone monomethyl ether (MEHQ, 4-methoxyphenol), 4-tert-butylcatechol (TBC) and with basic alumina to remove the inhibitor. Polyhydroxyethyl methacrylate (HEMA, ophthalmic grade 99+%) from Polysciences was also filtered through layers of HQ and MEHQ inhibitor removers and basic alumina before use.

Synthesis: POEOMA and SiO_2-POEOMA grafted nanoparticles were synthesized using ATRP technique in presence of CuBr as catalyst and Bipyridyl as ligand. In case of POEOMA, ethyl 2-bromo-2-methylpropionate was used as the ATRP initiator. SiO_2-POEOMA grafted nanoparticles were synthesized by grafting from technique, where an ATRP initiator was grafted onto the Si particles prior to the polymerization. Complete details and synthesis procedure can be found in the literature published previously [5]. The chemical structure for the SiO_2-POEOMA nanocomposites is represented in Figure 1.

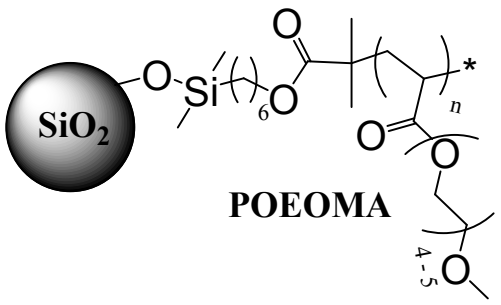

Figure 1. SiO_2-POEOMA chemical structure.

The purification of polymer-grafted nanoparticles followed a mixed solvent precipitation procedure to remove any remaining untethered or free chains. The dried sample was first redissolved in minimum amount of THF and centrifuged for 10 minutes. Unfunctionalized silica nanoparticles, if any, remained in the bottom of the tube and were readily separated from the bulk of the sample. The supernatant was then transferred to another flask and placed in an oil bath at 50 °C for 30 minutes. This step ensured the homogenous dispersion of the hybrid nanoparticles as well as any unattached chains in the solvent. The flask was then cooled down to room temperature. A non-solvent (acetone) was added dropwise to the solution until the cloudiness of the system persisted. After which, the flask was reheated to 50 °C resulting in a clear dispersion. The mixture was transferred to a separatory funnel and was left undisturbed for 2 days. The formation of two layers was observed. The bottom layer which contained the pure hybrid nanoparticles dispersed in THF was collected and precipitated in excess amount of acetone.

Determination of Polymer Molecular Weight by Size Exclusion Chromatography: In order to estimate the molecular weight of the synthesized polymers, size exclusion chromatography (SEC) measurements were carried out. Complete details can be found elsewhere [5]. From the SEC analysis, the number average molecular weight (M_n) for the POEOMA homopolymer and for the grafted POEOMA chains (chains cleaved from the SiO_2) were found to be 76.1 and 62.7 Kg/mol, respectively; with polydispersity indexes of 1.20 and 1.12, respectively.

Thermogravimetric Analysis of SiO_2-POEOMA Nanocomposites: Thermogravimetric analysis of SiO_2-POEOMA composites was performed on a TA Instruments TGA Q500 Thermogravimetric Analyzer under pure Ar flow. During the TGA analysis, the sample was heated to 1000 ^oC at 10 ^oC/min after an initial 10 minute isotherm at 30 ^oC and the weight loss of the nanocomposites upon heating was monitored. The nanocomposite samples were heated in vacuum oven at 55^oC overnight prior to TGA analysis. The SiO_2 content of the nanocomposites was estimated to be 3.0 ± 0.2 wt%.

Small-Angle X-Ray Scattering (SAXS): Small angle x-ray scattering (SAXS) measurements were performed using a Rigaku S-MAX3000 x-ray scattering apparatus with a 1.2 kW microfocus source and equipped with a two-dimensional multiwire detector. The q-scale was calibrated using a silver behenide standard. Samples were loaded between mylar sheets and the intensity data corrected for detector dark current and empty cell scattering at 30 ^oC.

Small-Angle Neutron Scattering (SANS): SANS experiments were carried out on the Bio-SANS instrument at the High Flux Isotope Reactor of Oak Ridge National Laboratory. Measurements were carried out at room temperature in 1.0 mm path quartz cuvettes. Scattering data and the associated backgrounds were recorded using multiple detector distances, specifically 14.5m, 6m and 0.3 m. The wavelength was set to 6 Å with a wavelength spread, $\Delta\lambda/\lambda$, of 0.15. The detector settings provide scattering vectors (q) $0.003 < q < 0.3$ Å, which allowed sufficient angular coverage to enable effective estimation of the incoherent scattering and accurate background subtraction. Some measurements were also carried out on the NGB 30m SANS beamline at the National Institute of Standards and Technology Center for Neutron Research (NCNR) in Gaithersburg, MD. The measurements were performed with a neutron wavelength of 6 Å and two sample-to-detector distances of 4m and 1m, thus accessing a q-range of 0.008 $Å^{-1}$ to

0.5 $Å^{-1}$. Data reduction followed standard procedures to correct for dark current, detector response, transmission and sample incoherent scattering background prior to azimuthal averaging to produce the 1-dimensional scattering profile at 30 ^{o}C [36].

Results and Discussion

Before describing the results of the structural characterization of the POEOMA based silica hybrids, we present the dilute solution (in 100% D_2O) SANS characterization of POEOMA with a similar molecular weight (~76 Kg/mol) to that present in the SiO_2-POEOMA nanocomposites samples, in Figure 2. The excluded volume model (see Supporting information material, Figure S.1.) was applied in order to calculate radius of gyration (R_g) of the POEOMA chains in D_2O; in Figure 2 the solid lines represent the fitting to the SANS experimental data for 1 and 2 wt.% POEOMA solutions. From the excluded volume model an R_g of 80 ± 3 Å was found. Additionally, Table S.1 (see the supporting information) shown the different R_g values obtained for the POEOMA homopolymer employing different models. It needs to be noted, that this average R_g value will be used in order to obtain the stretching ratio between the homopolymer free-chains and the grafted-chains within the nanoparticles.

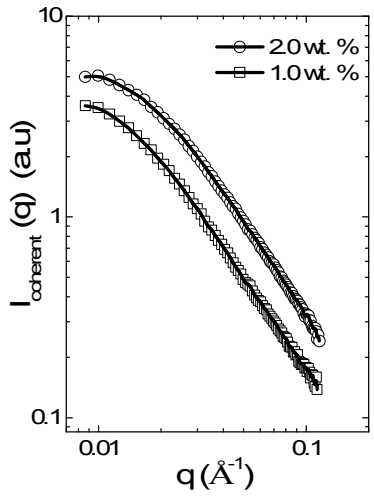

Figure 2. SANS scattering data for the POEOMA homopolymer, in 100 vol.% D_2O at a temperature of 30 ^oC. Solid lines represent the fitting to the Excluded Volume model.

The melt-state scattering behavior of the pure SiO_2-POEOMA hybrid as measured by small angle x-ray scattering is shown in Figure 3. The SAXS data were fitted using a hard sphere model with a log-normal distribution for the nanoparticle size, and indicated consistency with structure that was a *FCC* lattice with a weak presence of both first and second order intensity peaks (q_1^*:q_2^* :: 1:√3) (see Figure 3) [24]. The data described here is similar to that observed for other multi-arm star systems most notably the pioneering work of Vlassapoulos [37, 38], wherein they demonstrated similar scattering signatures from assemblies of multi-arm stars in the melt and in solutions. From this fitting the mean diameter of the silica nanoparticle was found to be D ~ 14.6 ± 0.5 nm (R ~ 7.3 ± 0.25 nm), with the presence of an ordered structure with a mean distance between silica nanoparticles ~ 45.3 ± 0.5 nm (center-to-center distance). We note that the mean shell-to-shell distance is ~ 30.7 ± 1 nm, a value significantly larger than twice the unperturbed radius of gyration of comparable dilute free chains in water; this suggests that the grafted POEOMA chains are significantly stretched in such hybrids due to the grafting of such chains at high grafting density on the silica nanoparticles.

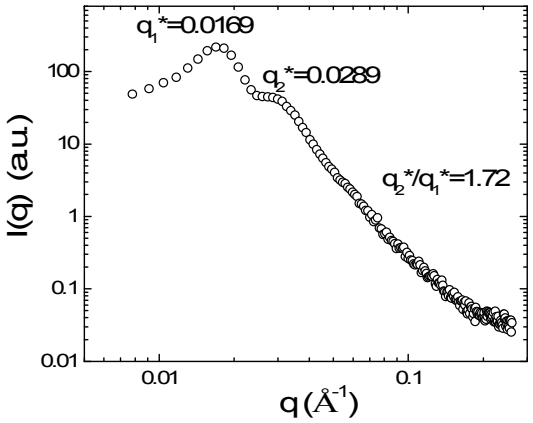

Figure 3. SAXS data for a bulk sample of SiO_2-POEOMA nanoparticle hybrids at 30 ^oC, where the POEOMA chains are in their melt state.

Figure 4 shows the SANS data for low wt. % SiO_2-POEOMA hybrid dispersions in water (low concentration regime: from 0.1 to 2 wt.%). It is clearly visible that the data over these concentrations, we observe only the individual contributions from the hybrid material, *i.e.,* the inter-particles interactions (structure factor) are absent and the hybrid structure did not alter as a function of concentration. This can also be observed when the intensity is normalized by the volume fraction of scatterers and the data superpose over a broad concentration range as shown in Figure 4 [39]. Evaluating SiO_2-POEOMA wt. % equal or lower than 2% will allow us to estimate only the neat structure (form factor) of individual scatters.

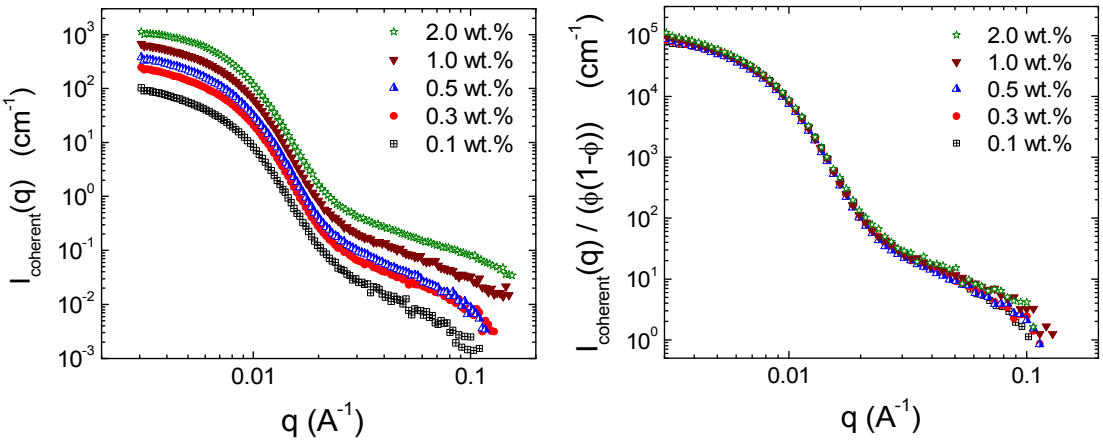

Figure 4. SANS intensity scattering profiles (30°C) in D_2O, for SiO_2-POEOMA samples in the low concentration regime: (left) original experimental data of scattered intensity as a function of wavevector; (right) volume-corrected profiles.

In neutron scattering, contrast variation method is used to isolate features of complex structures (*i.e.,* separate the scattering contributions of core from the shell in a core-shell like structure)[40, 41]. This can be achieved because hydrogen and deuterium have very different neutron scattering length densities (SLDs, denoted ρ_i for component i) characterizing the way they interact with neutrons (*i.e.,* for H_2O and D_2O the SLDs are -5.6×10^{-7} Å^{-2} and 6.3×10^{-6} Å^{-2}, respectively). In our SANS experiments, we consider that the SLD of a mixture (D_2O/H_2O) is a volume fraction weighted average of the SLDs of the individual components, allowing the SLD

of a mixed solvent system to be determined. Table 2 summarizes the coherent neutron scattering length densities for all the materials employed in this work.

Table 2. Coherent Neutron Scattering Length Densities (ρ)

Material	ρ (Å^{-2})
H_2O	-5.6×10^{-7}
D_2O	6.3×10^{-6}
SiO_2	3.4×10^{-6}
POEOMA	8.3×10^{-7}

The results of a contrast variation SANS study of a 2 wt.% SiO_2-POEOMA sample in mixtures of H_2O and D_2O are presented in Figure 5. We note that the scattering intensity decreased with decreased D_2O content in the solvent mixture until about 25 % D_2O. For the dispersions of SiO_2-POEOMA hybrids in solvents, there are multiple contrasts (SiO_2 with solvent and POEOMA with solvent) and therefore a single match point does not exist. In order to demonstrate the presence of multiple contrast match points (between the core and shell constituents with the solvent), the intensities at selected q value were evaluated as a function of D_2O fraction as seen in Figure 6. At a lower q value (q = 0.007 Å) only a single contrast match point can be observed at 25 vol. % D_2O, which can be assigned to the POEOMA chains match point (in close agreement with theoretical calculations shown in Figure S.2). In this case, the scattering contribution originating from the SiO_2 core will be observed. On the other hand, at a higher q value (q = 0.1 Å), two contrast minima points are clearly visible: the first one at 25 vol% D_2O which has been already assigned to the POEOMA chains and the second one at 40 vol. % D_2O that is assigned to the SiO_2 contrast match point. While the experimentally measured contrast match point for the polymer agrees closely to the theoretical calculated value (Fig S2)

that is not the case for the contrast match point corresponding to the SiO_2 core. This presumably originates from a dense polymer chain layer close to the SiO_2 particles that essentially behave as dense hard sphere and thus reduce the core SLD (2.18 $x10^{-6}$ A^{-2} opposed to the value for silica of ~ $3.4x10^{-6}$ A^{-2}). Figure 5 allowed us to therefore assign contrast matching for the different portions (SiO_2 particles and POEOMA chains) and also it indicated that the total scattering intensity, in different *q* ranges, was dominated by different portions within the hybrid material.

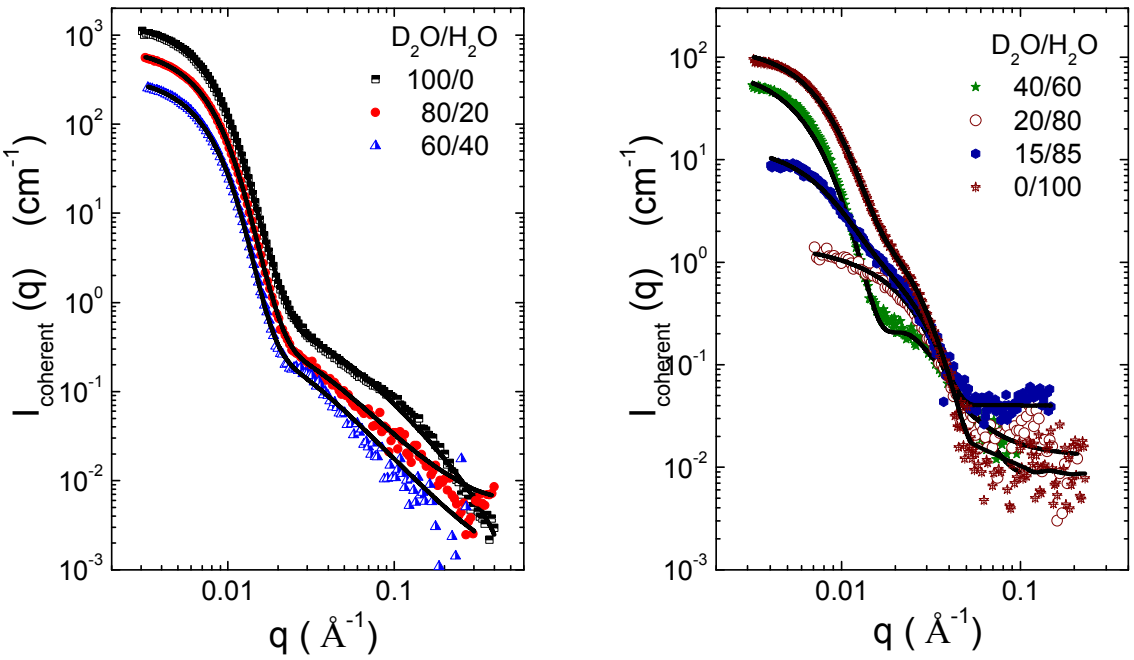

Figure 5. SANS scattering curves (at 30°C) for a 2 wt% SiO_2-POEOMA sample, in different D_2O/H_2O ratio solutions: (left) curves fitted with the Fuzzy Sphere model and, (right) curves fitted with the Core-Shell model.

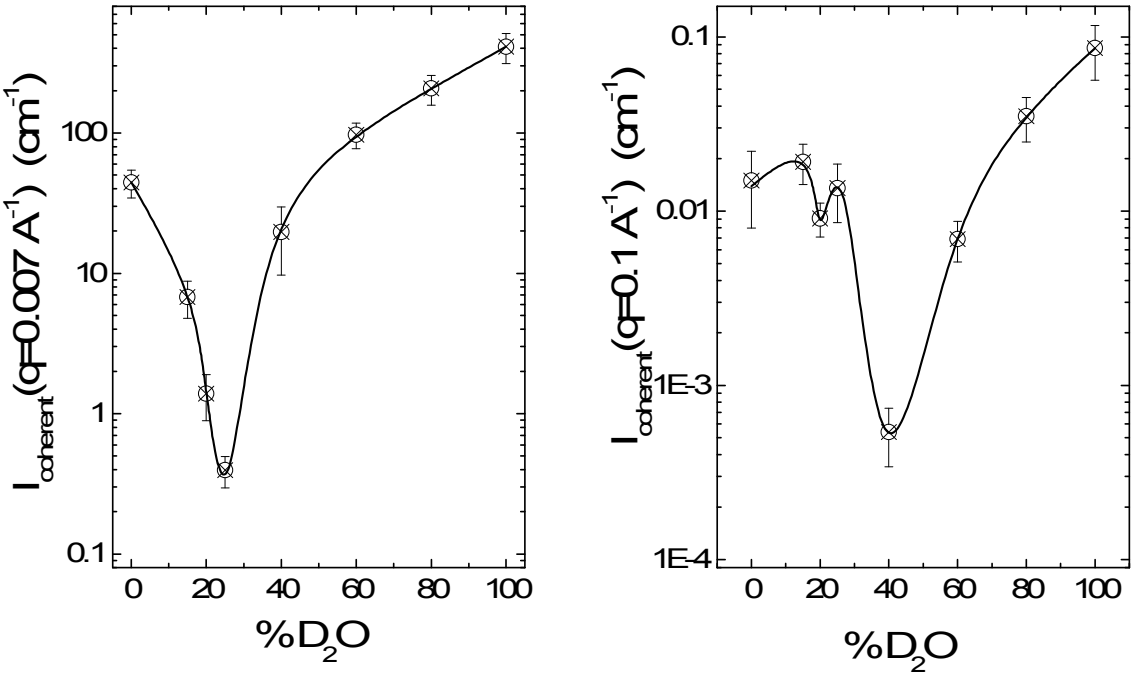

Figure 6. Scattering intensities at two different *q* values as function of the % D_2O content for a 2 wt % SiO_2 – POEOMA sample.

In order to evaluate the structural characteristics of the SiO_2-POEOMA hybrids, the SANS scattering data were modeled using a fuzzy sphere model [27, 42, 43] and a spherical core-shell model [40, 42]. The core-shell model considers spherical particles having a polydisperse core (and in this case with a fixed SLD) with a shell thickness of constant thickness. The form factor is normalized by the average particle volume fraction. This model appeared to be most relevant when there was poor contrast between the outer polymer shell and the solvent, where effectively the exterior shell of the polymer was no longer clearly observed. On the other hand, the fuzzy sphere model was also used to model the data as it is able to calculate the scattering intensity from spherical particles with a "fuzzy" interface. In this model a Gaussian distribution of the particle radii is assumed and combined with a Lorentzian term that accounts for the fluctuations of the shell (grafted chains) density, with the radial density profile decreased gradually from the sphere surface [27, 43]. This model appeared to be most representative of the system wherein the

polymer in the outer shell has a large contrast with the solvent and the silica particle (with the inner dense shell of the polymer) and the scattering measurements probed the entire structure of the hybrid nanoparticles.

For the hybrid samples considered here, in the swollen state the polymer segment density of a particle can be estimated to be not homogenously distributed but gradually decrease from the core through the shell surface, a schematic particle model can be seen in Figure 7. This structure is consistent with the model proposed by Daoud and Cotton [44], verified for block copolymer micelles[32] and subsequently for multi-arm stars [38]. Interestingly, the region close to the nanoparticles is largely impenetrable to the solvent, a reflection of the high density of chains at the interface. We anticipate that this region will change with change in the thermodynamic character of the solvent and has been studied for the case a polymer matrix with changing phase behavior with the grafted chains [35].

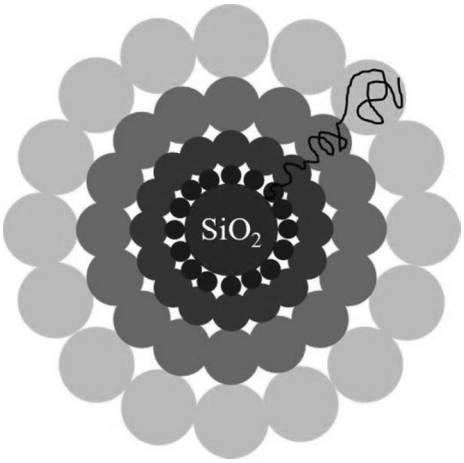

Figure 7. Proposed particle model for the SiO_2-POEOMA nanoparticles. Due to the POEOMA grafting density at the core surface, a decreasing gradient density will be presented from the SiO_2 core through the shell surface (darker to lighter color in the scheme).

As noted in Figure 5, the fuzzy sphere model fits well when the D_2O content is equal or higher than 60 vol. % (high D_2O content systems). For lower D_2O concentrations, the fitting to the fuzzy sphere model deviates noticeably. In those cases, *i.e.,* for D_2O content equal to or lower

than 40 vol. %, the core-shell model was successfully applied (see Figure 5, right). The contrast variation results shown in Figure 5, provide an unequivocal methodology to understand quantitatively the structure of the polymer chains when tethered to the silica nanoparticles and lend support to previous reports on bottlebrush and grafted polymer structures [22, 26, 28, 45].

Using the average SiO_2 core radius (from the SAXS analysis) and the fitting parameter from the employed SANS model fit, the thickness of the POEOMA shell can be obtained. We identify two main components in the hybrid structure: i) a dense hybrid core, which is formed by the SiO_2 core surrounded by a dense POEOMA shell, where the polymer chains are poorly solvated solvated by the solvent, and; ii) the nanoparticle shell, which essentially is formed by a less dense POEOMA chains and strongly solvated by the solvent. The two most critical data sets to consider are those at 40 % D_2O where the solvent SLD is close to the SLD of the silica-dense polymer hybrid core and the data set at 25% D_2O where the solvent SLD is close to that of the outer shell of the polymer chains. We note that the data for the 40 % D_2O sample indicates that the chains attached to the silica nanoparticle are highly stretched compared to the solution scattering data described in Figure 2 for the free polymer chains in water.

From the fitted values, a stretching ratio value could be calculated using the following equation:

$$R_{stretching} = \frac{(hybrid\ core\ radius\ +\ shell\ thickness\ -\ SiO_2\ radius_{(SAXS)})}{R_g} \qquad \text{(eq. 1)}$$

with the underlying assumption that there is no interpenetration of chains in the shell layers. Table 3 presents the POEOMA hybrid core radius, the shell thickness (t) and the stretching ratio for the 2 wt % SiO_2-POEOMA nanocomposite in D_2O/H_2O mixture with higher D_2O content.

Table 3. Fitting values and the stretching ration for the SiO_2-POEOMA nanocomposite in different D_2O/H_2O mixtures, at 30°C.

D_2O vol. %	Hybrid Core Radius (Å)	Shell thickness (Å)	$R_{stretching}$	SLD Shell (A^{-2})	SLD Solvent (A^{-2})
Fuzzy Sphere model					
100	181 ± 21	67 ± 5	2.2 ± 0.4	3.26 (±0.1) x10^{-6}	6.30 x10^{-6}
80	165 ± 18	78 ± 4	2.1 ± 0.2	2.54 (±0.3) x10^{-6}	4.93 x10^{-6}
60	178 ± 20	87 ± 6	2.4 ± 0.3	1.89 (±0.2) x10^{-6}	3.56 x10^{-6}
Core-Shell model					
40	91 ± 11	133 ± 7	2.1 ± 0.3	1.25 (±0.2) x10^{-6}	2.18 x10^{-6}
25	88 ± 4	7 ± 3		1.14 (±0.2) x10^{-6}	1.16 x10^{-6}
20	84 ± 6	5 ± 4		1.08 (±0.6) x10^{-6}	8.27 x10^{-7}
15	88 ± 4	7 ± 3		1.85 (±0.5) x10^{-6}	4.69 x10^{-7}
0	94 ± 9	101 ± 13	1.6 ± 0.4	2.60 (±0.4) x10^{-6}	-5.60 x10^{-7}

From the extracted fitting parameters presented in Table 3, we infer from the conditions where the solvent mixture SLD is different from the POEOMA contrast match point (15~25 vol%. D_2O), that the POEOMA chains are stretched at least two times when grafted to the SiO_2 nanoparticles. For the conditions where the SLD of the solvent mixture is close to that of the POEOMA outer shell, the scattering models do not provide an accurate measure of the shell thickness and therefore a value of $R_{stretching}$ could not be obtained. Moreover, the extracted core radius obtained from SANS data fitting is slightly larger than the same obtained from SAXS measurements and consistent with the notion of a non-solvated polymer shell in proximity to the SiO_2 surface.

Figure 8 shows how the structure factor became more evident at higher nanoparticles concentrations. Using a spherical core-shell form factor (*P(q)*) combined with a hard sphere (HS) structure factor (*S(q)*) with a Percus-Yevick (PY) closure, it was possible to obtain reasonable fits for the scattering intensity ($I(q) = k\ P(q)\ S(q)$) from 3, 5 and 10 wt.% SiO_2-POEOMA nanoparticles at the POEOMA match point (25/75 D_2O/H_2O). Working close to the POEOMA contrast match point greatly reduced the scattering contribution originating from the POEOMA

chains. The applicability of a hard-sphere structure factor implies that the dense cores (of the SiO_2 – polymer inner shell) in these dilute to semi-dilute solutions interact through volume exclusion. From those fitting an average SiO_2 radius was found to be around 8.3 ± 0.5 nm, a value in close agreement with the result found using the bulk sample SAXS scattering and the lower concentration Core-Shell modelling demonstrated in Table 3.

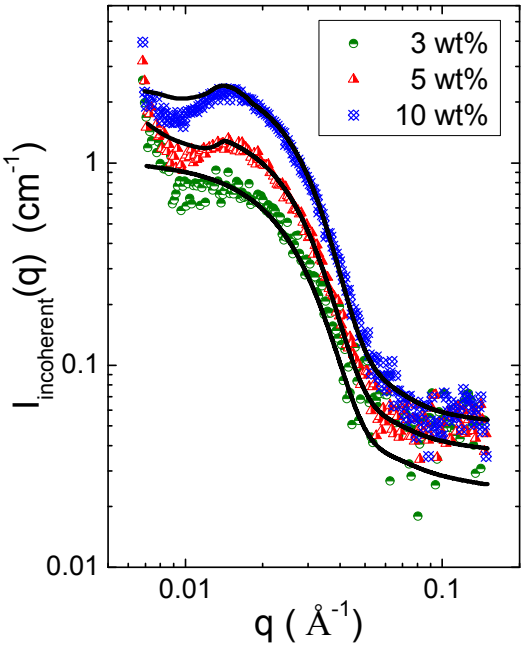

Figure 8. SANS intensity scattering profiles, 30°C, for SiO_2-POEOMA samples, in the high hybrid concentration regime, at 25/75 D_2O/H_2O. The Percus-Yevick approximation provides excellent agreement with the observed intensity data and indicates that under conditions where the polymer shell is contrast matched, the particles interact with each other through hard-sphere like interactions.

Conclusions

Contrast variation based small-angle neutron scattering of dilute dispersions of a POEOMA – SiO_2 nanoparticle hybrids is an excellent tool to understand the structure of the polymer chains when they are attached at high grafting densities to the nanoparticle. The tethered polymer chains are highly stretched compared to the dimensions of the free chains

dissolved in the same solvent. Moreover, the scattering data from higher concentration dispersions of the nanoparticles, under conditions where the solvated polymer chain based outer shell is contrast matched by the solvent, demonstrate good agreement with a Percus-Yevick approximation to describe the interactions between nanoparticles.

These characterization methods, and the presence of two distinct contrast minimum ratios of solvent isotopic mixtures corresponding to the matching of the contrast with the outer shell and the inner core with the solvent, indicates that these methods can be used to characterize the interactions between the brush chains with each other as well as with the solvent and therefor enable unique molecular level detail of the characterization of thermodynamic transitions. Specifically, we believe that the issues of dewetting of the polymer brush and the phase transition resulting from the incompatibility of the polymer brush and the matrix solvent or polymers would be ideally suited for such a study [31, 35].

Acknowledgement

SAXS data were obtained using an instrument obtained on a National Science Foundation (NSF DMR 1040446) funded instrument. A portion of this research at ORNL's High Flux Isotope Reactor was sponsored by the Scientific User Facilities Division, Office of Basic Energy Sciences, US Department of Energy. A portion of this work utilized the NIST Center for Neutron Research (NCNR) supported in part by the National Science Foundation under Grant #DMR-0944772.

References:

1. V. Ganesan and A. Jayaraman, *Soft Matter*, 2014, **10**, 13-38; S. K. Kumar, N. Jouault, B. Benicewicz and T. Neely, *Macromolecules*, 2013, **46**, 3199-3214.

2. V. Goel, T. Chatterjee, L. Bombalski, K. Yurekli, K. Matyjaszewski and R. Krishnamoorti, *J. Polym. Sci. Pt. B-Polym. Phys.*, 2006, **44**, 2014-2023.

3. S. Nayak and L. A. Lyon, *Angewandte Chemie International Edition*, 2004, **43**, 6706-6709.

4. J. Pyun and K. Matyjaszewski, *Chemistry of Materials*, 2001, **13**, 3436-3448.

5. R. Ponnapati, O. Karazincir, E. Dao, R. Ng, K. K. Mohanty and R. Krishnamoorti, *Ind. Eng. Chem. Res.*, 2011, DOI: 10.1021/ie2019257.

6. Y.-P. Wang, X.-W. Pei, X.-Y. He and K. Yuan, *European Polymer Journal*, 2005, **41**, 1326-1332.

7. O. Prucker and J. Ruhe, *Macromolecules*, 1998, **31**, 602-613; O. Prucker and J. Ruhe, *Macromolecules*, 1998, **31**, 592-601; X. Fan, C. Xia and R. C. Advincula, *Langmuir*, 2003, **19**, 4381-4389; T. Stohr and J. Ruhe, *Macromolecules*, 2000, **33**, 4501-4511.

8. O. Webster, *Science*, 1991, **251**, 887-893.

9. J.-S. Wang and K. Matyjaszewski, *Journal of the American Chemical Society*, 1995, **117**, 5614-5615; K. Matyjaszewski and J. Xia, *Chemical Reviews*, 2001, **101**, 2921-2990; M. Kamigaito, T. Ando and M. Sawamoto, *Chemical Reviews*, 2001, **101**, 3689-3746.

10. D. M. Jones, A. A. Brown and W. T. S. Huck, *Langmuir*, 2002, **18**, 1265-1269; W. Huang, J.-B. Kim, M. L. Bruening and G. L. Baker, *Macromolecules*, 2002, **35**, 1175-1179; W. Huang, G. L. Baker and M. L. Bruening, *Angewandte Chemie International Edition*, 2001, **40**, 1510-1512.

11. X. Chen, D. P. Randall, C. Perruchot, J. F. Watts, T. E. Patten, T. von Werne and S. P. Armes, *Journal of Colloid and Interface Science*, 2003, **257**, 56-64; J. N. Kizhakkedathu and D. E. Brooks, *Macromolecules*, 2003, **36**, 591-598; P. von Natzmer, D. Bontempo and N. Tirelli, *Chemical Communications*, 2003, 1600-1601; G. Zheng and H. D. H. Stöver, *Macromolecules*, 2003, **36**, 1808-1814; T. von Werne and T. E. Patten, *Journal of*

the American Chemical Society, 1999, **121**, 7409-7410; J. Pyun, S. Jia, T. Kowalewski, G. D. Patterson and K. Matyjaszewski, *Macromolecules*, 2003, **36**, 5094-5104; P. Liu, W. Liu and Q. Xue, *Journal of Macromolecular Science, Part A: Pure and Applied Chemistry*, 2004, **41**, 1001 - 1010.

12. T. Ishizone, A. Seki, M. Hagiwara, S. Han, H. Yokoyama, A. Oyane, A. Deffieux and S. Carlotti, *Macromolecules*, 2008, **41**, 2963-2967.

13. H. Hussain, K. Y. Mya and C. He, *Langmuir*, 2008, **24**, 13279-13286.

14. J. F. Lutz, *Journal of Polymer Science Part a-Polymer Chemistry*, 2008, **46**, 3459-3470; J. F. Lutz and A. Hoth, *Macromolecules*, 2006, **39**, 893-896.

15. C. R. Becer, S. Hahn, M. W. M. Fijten, H. M. L. Thijs, R. Hoogenboom and U. S. Schubert, *Journal of Polymer Science Part A: Polymer Chemistry*, 2008, **46**, 7138-7147.

16. Y. Li, R. Liu, W. Liu, H. Kang, M. Wu and Y. Huang, *Journal of Polymer Science Part A: Polymer Chemistry*, 2008, **46**, 6907-6915.

17. J. P. Magnusson, A. Khan, G. Pasparakis, A. O. Saeed, W. Wang and C. Alexander, *Journal of the American Chemical Society*, 2008, **130**, 10852-10853.

18. H. Tai, W. Wang, T. Vermonden, F. Heath, W. E. Hennink, C. Alexander, K. M. Shakesheff and S. M. Howdle, *Biomacromolecules*, 2009, **10**, 822-828.

19. N. Fechler, N. Badi, K. Schade, S. Pfeifer and J.-F. o. Lutz, *Macromolecules*, 2008, **42**, 33-36; N. Badi and J.-F. Lutz, *Journal of Controlled Release*, 2009, **140**, 224-229.

20. S. Rose, A. Marcellan, T. Narita, F. Boue, F. Cousin and D. Hourdet, *Soft Matter*, 2015, **11**, 5905-5917.

21. C. J. Kim, M. Kraska, M. Mazurowski, K. Sondergeld, M. Gallei, M. Rehahn and B. Stuhn, *Soft Materials*, 2014, **12**, S41-S48; V. Lebedev, G. Torok and L. Vinogradova, *Journal of Macromolecular Science Part B-Physics*, 2013, **52**, 1736-1755; C. J. Kim, K. Sondergeld, M. Mazurowski, M. Gallei, M. Rehahn, T. Spehr, H. Frielinghaus and B. Stuhn, *Colloid Polym. Sci.*, 2013, **291**, 2087-2099; M. J. A. Hore, J. Ford, K. Ohno, R. J. Composto and B. Hammouda, *Macromolecules*, 2013, **46**, 9341-9348; F. Gal, H. Perez, V. Noel and G. Carrot, *Journal of Polymer Science Part a-Polymer Chemistry*, 2012, **50**,

289-296; V. Goel, J. Pietrasik, K. Matyjaszewski and R. Krishnamoorti, *Ind. Eng. Chem. Res.*, 2010, **49**, 11985-11990.

22. C. Chevigny, D. Gigmes, D. Bertin, J. Jestin and F. Boue, *Soft Matter*, 2009, **5**, 3741-3753.

23. D. Kim and R. Krishnamoorti, *Ind. Eng. Chem. Res.*, 2015, **54**, 3648-3656.

24. V. Goel, J. Pietrasik, H. C. Dong, J. Sharma, K. Matyjaszewski and R. Krishnamoorti, *Macromolecules*, 2011, **44**, 8129-8135.

25. C. E. Estridge and A. Jayaraman, *J. Polym. Sci. Pt. B-Polym. Phys.*, 2015, **53**, 76-88; M. Asai, A. Cacciuto and S. K. Kumar, *Soft Matter*, 2015, **11**, 793-797; T. B. Martin and A. Jayaraman, *J. Polym. Sci. Pt. B-Polym. Phys.*, 2014, **52**, 1661-1668; B. Lin, T. B. Martin and A. Jayaraman, *ACS Macro Letters*, 2014, **3**, 628-632; J. Moll, S. K. Kumar, F. Snijkers, D. Vlassopoulos, A. Rungta, B. C. Benicewicz, E. Gomez, J. Ilavsky and R. H. Colby, *ACS Macro Letters*, 2013, **2**, 1051-1055; T. B. Martin and A. Jayaraman, *Soft Matter*, 2013, **9**, 6876-6889; T. B. Martin and A. Jayaraman, *Macromolecules*, 2013, **46**, 9144-9150; A. Jayaraman, *J. Polym. Sci. Pt. B-Polym. Phys.*, 2013, **51**, 524-534; P. M. Dodd and A. Jayaraman, *J. Polym. Sci. Pt. B-Polym. Phys.*, 2012, **50**, 694-705; D. Maillard, S. K. Kumar, A. Rungta, B. C. Benicewicz and R. E. Prud'homme, *Nano Lett.*, 2011, **11**, 4569-4573; L. M. Hall, A. Jayaraman and K. S. Schweizer, *Curr. Opin. Solid State Mat. Sci.*, 2010, **14**, 38-48; P. Akcora, H. Liu, S. K. Kumar, J. Moll, Y. Li, B. C. Benicewicz, L. S. Schadler, D. Acehan, A. Z. Panagiotopoulos, V. Pryamitsyn, V. Ganesan, J. Ilavsky, P. Thiyagarajan, R. H. Colby and J. F. Douglas, *Nat. Mater.*, 2009, **8**, 354-U121.

26. J. Kalb, D. Dukes, S. K. Kumar, R. S. Hoy and G. S. Grest, *Soft Matter*, 2011, **7**, 1418-1425.

27. M. Stieger, W. Richtering, J. S. Pedersen and P. Lindner, *Small-angle neutron scattering study of structural changes in temperature sensitive microgel colloids*, AIP, 2004.

28. M. J. A. Hore, X. C. Ye, J. Ford, Y. Z. Gao, J. Y. Fei, Q. Wu, S. J. Rowan, R. J. Composto, C. B. Murray and B. Hammouda, *Nano Lett.*, 2015, **15**, 5730-5738; C. Picot, F. Audouin and C. Mathis, *Macromolecules*, 2007, **40**, 1643-1656.

29. Y. Jiao and P. Akcora, *Phys. Rev. E*, 2014, **90**, 9; G. G. Vogiatzis and D. N. Theodorou, *Macromolecules*, 2013, **46**, 4670-4683; H. Lee, D. H. Kim, K. N. Witte, K. Ohn, J. Choi, B. Akgun, S. Satija and Y. Y. Won, *J. Phys. Chem. B*, 2012, **116**, 7367-7378; S. Lecommandoux, F. Checot, R. Borsali, M. Schappacher, A. Deffieux, A. Brulet and J. P. Cotton, *Macromolecules*, 2002, **35**, 8878-8881.

30. M. Mazurowski, K. Sondergeld, J. Elbert, C. J. Kim, J. Y. Li, H. Frielinghaus, M. Gallei, B. Stuhn and M. Rehahn, *Macromol. Chem. Phys.*, 2013, **214**, 1094-1106.

31. M. Zackrisson, A. Stradner, P. Schurtenberger and J. Bergenholtz, *Langmuir*, 2005, **21**, 10835-10845.

32. R. Krishnamoorti, S. Rai and M. B. Shek, *Soft Materials*, 2003, **1**, 263-275.

33. M. Moffitt, Y. S. Yu, D. Nguyen, V. Graziano, D. K. Schneider and A. Eisenberg, *Macromolecules*, 1998, **31**, 2190-2197; L. Willner, O. Jucknischke, D. Richter, B. Farago, L. J. Fetters and J. S. Huang, *Europhys. Lett.*, 1992, **19**, 297-303.

34. M. A. J. Gillissen, T. Terashima, E. W. Meijer, A. R. A. Palmans and I. K. Voets, *Macromolecules*, 2013, **46**, 4120-4125; O. V. Borisov, E. B. Zhulina and T. M. Birshtein, *Acs Macro Letters*, 2012, **1**, 1166-1169; D. Potschke, M. Ballauff, P. Lindner, M. Fischer and F. Vogtle, *Macromol. Chem. Phys.*, 2000, **201**, 330-339.

35. T. B. Martin, K. I. S. Mongcopa, R. Ashkar, P. Butler, R. Krishnamoorti and A. Jayaraman, *Journal of the American Chemical Society*, 2015, **137** 10624-10631.

36. S. R. Kline, *J Appl Crystallogr*, 2006, **39**, 895-900; C. J. Glinka, J. M. Nicol, G. D. Stucky, E. Ramli, D. Margolese, Q. Huo, J. B. Higgins and M. E. Leonowicz, *J Porous Mat*, 1996, **3**, 93-98.

37. D. Vlassopoulos, G. Fytas, J. Roovers, T. Pakula and G. Fleischer, *Faraday Discuss.*, 1999, **112**, 225-235; R. Seghrouchni, G. Petekidis, D. Vlassopoulos, G. Fytas, A. N. Semenov, J. Roovers and G. Fleischer, *Europhys. Lett.*, 1998, **42**, 271-276; D. Vlassopoulos, T. Pakula, G. Fytas, J. Roovers, K. Karatasos and N. Hadjichristidis, *Europhys. Lett.*, 1997, **39**, 617-622.

38. T. Pakula, D. Vlassopoulos, G. Fytas and J. Roovers, *Macromolecules*, 1998, **31**, 8931-8940.

39. A. P. Gast, *Langmuir*, 1996, **12**, 4060-4067; C. M. Stancik, A. R. Lavoie, P. A. Achurra, R. M. Waymouth and A. P. Gast, *Langmuir*, 2004, **20**, 8975-8987; C. M. Stancik, A. R. Lavoie, J. Schütz, P. A. Achurra, P. Lindner, A. P. Gast and R. M. Waymouth, *Langmuir*, 2003, **20**, 596-605.

40. A. Ramzi, Rijcken, Veldhuis, D. Schwahn, W. E. Hennink and C. F. van Nostrum, *The Journal of Physical Chemistry B*, 2008, **112**, 784-792.

41. J. S. B. Higgins, H., ed., *Polymers and Neutrons Scattering*, Clarendon Press, Oxford, U.K., 1994; M. Zackrisson, A. Stradner, P. Schurtenberger and J. Bergenholtz, *Langmuir*, 2005, **21**, 10835-10845; C. D. Jones and L. A. Lyon, *Macromolecules*, 2000, **33**, 8301-8306.

42. I. Berndt, J. S. Pedersen and W. Richtering, *Angewandte Chemie International Edition*, 2006, **45**, 1737-1741.

43. M. Stieger, J. S. Pedersen, P. Lindner and W. Richtering, *Langmuir*, 2004, **20**, 7283-7292.

44. M. Daoud and J. P. Cotton, *Journal de Physique* 1982, **43**, 531-538.

45. C. Chevigny, D. Gigmes, D. Bertin, R. Schweins, J. Jestin and F. Boue, *Polymer Chemistry*, 2011, **2**, 567-571.

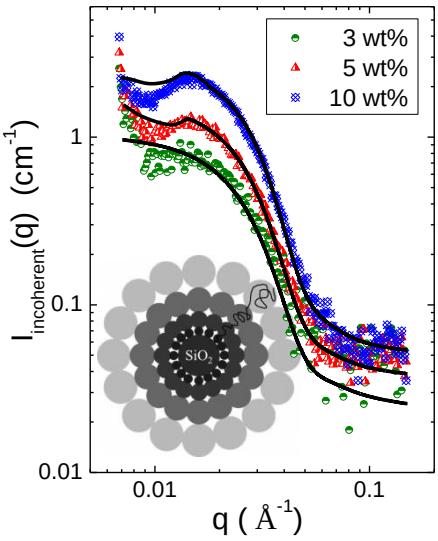
3 wt%
5 wt%
10 wt%
$I_{incoherent}(q)$ (cm^{-1})
1
0.1
0.01
0.01
0.1
q (Å^{-1})
SiO_2
PDMS